

Jeff Head received his B.S. in chemistry from Colorado State University in the spring of 2006. As an undergraduate Jeff worked with Dr. Bruce Parkinson in a combinatorial analysis of metal oxides capable of driving the water-splitting reaction for hydrogen production. Before and after senior year at CSU Jeff completed two Science Undergraduate Laboratory Internships (SULI) at the National Renewable Energy Laboratory (NREL). While at NREL the focus of his studies were to carry out the photoelectrochemical characterization of various nitride compounds. Specifically, the goal of the research was to determine the water-splitting capabilities of the compounds with light as the only energy input. Advising him on the project was Dr. John Turner (NREL). He is currently pursuing graduate studies in analytical chemistry at the University of Arizona for his PhD.

John A. Turner is a Principal Scientist at the National Renewable Energy Laboratory. He received his B.S. from Idaho State University, his PhD from Colorado State University, and completed a postdoctoral appointment at the California Institute of Technology before joining the Laboratory (then the Solar Energy Research Institute) in 1979. His research is primarily concerned with enabling technologies for the implementation of hydrogen systems into the energy infrastructure. This includes direct conversion (photoelectrolysis) systems for hydrogen production from sunlight and water, advanced materials for high temperature fuel cell membranes, and corrosion studies of fuel cell metal bipolar plates.

## SILICON NITRIDE FOR DIRECT WATER-SPLITTING AND CORROSION MITIGATION

JEFF HEAD, JOHN A. TURNER

### ABSTRACT

Today's fossil fuels are becoming harder to obtain, creating pollution problems, and posing hazards to people's health. One alternative to fossil fuels is hydrogen, capable of serving as a clean and efficient energy carrier. Certain semiconductors are able to harness the energy of photons and direct it into water electrolysis in a process known as photoelectrochemical water splitting. Triple junction devices integrate three semiconductors of different band gaps resulting in a monolithic material that absorbs over a broader spectrum. Amorphous silicon (a-Si) is one such material that, when stacked in tandem, possesses water-splitting capabilities. Even though a-Si is capable of splitting water, it is an unstable material in solution and therefore requires a coating to protect the surface from corrosion. A stable, transparent material that has the potential for corrosion protection is silicon nitride. In this study, silicon nitride thin films were grown using DC magnetron sputtering with varying amounts of argon and nitrogen added to the system. X-ray diffraction indicated amorphous silicon nitride films. Current as a function of potential was determined from cyclic voltammetry measurements. Mott-Schottky analysis showed n-type behavior with absorption and transmission measurements indicated variation in flatband potentials. Variation in band gap values ranging from 1.90 to 4.0 eV. Corrosion measurements reveal that the silicon nitride samples exhibit both p-type and n-type behavior. Photocurrent over a range of potentials was greater in samples that were submerged in acidic electrolyte. Silicon nitride shows good stability in acidic, neutral, and basic solutions, indicative of a good material for corrosion mitigation.

### INTRODUCTION

Energy resources have and always will be a cause for concern in order to meet the energy needs and requirements that society deals with in everyday life. To date, most of the world's energy is obtained from fossil fuels, nuclear power, and renewable processes from the power of the sun and wind. However, pollution from fossil fuels used to power today's society create many environmental and health problems. Global warming is also linked to the exponentially increasing anthropogenic carbon dioxide concentrations in the atmosphere that has been taking place over the past 200 years [1]. Hydrogen fuel can be obtained from biomass conversion or using any renewably generated electricity for water electrolysis. Renewably

produced hydrogen is a clean and efficient way of storing energy harnessed through typically intermittent renewable technologies such as wind, and solar power.

One of the most efficient ways of producing hydrogen is using sunlight to directly split water into hydrogen and oxygen on semiconductor surfaces [2]. At least 1.23 V are required for splitting water into hydrogen and oxygen. A cathodic overpotential of 100 mV and an anodic overpotential of 200 mV means an efficient photoelectrolysis system should have a band gap of at least 1.53 eV, where band gaps above 2.0 eV absorb less of the solar spectrum [3]. Two other requirements for water splitting are stability of the semiconductor in solution and "straddling" of the redox potentials of the hydrogen and oxygen evolution reactions by the energy bands

[3]. Specifically, the energy bands must encompass the potentials at which the following half reactions occur:



Semiconductors are classified as either n-type or p-type. Semiconductors in which the majority charge carriers are electrons are n-type whereas those in which the majority charge carriers are holes are p-type [4]. Oxygen is produced on the surface of n-type materials and hydrogen on the surface of p-type materials. Preliminary characterization of semiconductors can be carried out with open circuit potential measurements, photocurrent measurements, and Mott-Schottky analysis [5]. In considering the location of the band edges one must factor in the Fermi level of the material, which for n-type materials lies just below the conduction band, and for p-type materials lies slightly above the valence band. The flatband potential, or the energy of the Fermi level when the bands are flat, can be estimated from Mott-Schottky plots [4], based on the equation

$$\frac{1}{C^2} = \frac{1.41 \times 10^{32}}{\epsilon N_D} \left[ E - (V_{fb}) \frac{kT}{e} \right] \quad (3)$$

where C is the capacity of the space charge layer,  $\epsilon$  is the static dielectric of the semiconductor, e is the electronic charge,  $N_D$  is the doping density, and E is the electrode potential [4]. Plotting the inverse square of capacitance versus voltage will give a linear plot with x-intercept equal to the flatband potential and a slope inversely proportional to the doping density.

Currently there exist solid-state multijunction devices that can generate the potential energy required for hydrogen and oxygen production from water while accessing a large fraction of the solar spectrum. For example, triple junction amorphous silicon (a-Si), devices can produce potentials greater than 1.8 V, sufficient for water-splitting and can be manufactured for maximum efficiency. However, a-Si exhibits a lack of stability when in solution, and therefore requires a protective coating. Previous studies have shown that the use of amorphous silicon carbide as a protective coating offers protection but attenuates too much light, thereby preventing maximum efficiency of hydrogen production by a-Si [6]. A possible solution is the use of silicon nitride which can offer the transparent qualities that silicon carbide lacks.

Previous work has shown that silicon nitride is a stable material, has transparent and nontransparent qualities, and its composition can be varied to be an absorber for the direct water splitting reaction itself [7]. With the ability to vary the composition of silicon nitride, and therefore the band gap of this material, it is the goal of this research to offer a transparent protective coating for a-Si, and thereby realize the USDOE 2005 goal of 7.5% solar to hydrogen efficiency and 1000 hours of stability. With the ability to vary the band gap of this compound, silicon nitride will also be considered for driving the water-splitting reaction as a single-gap device.

## MATERIALS AND METHODS

Silicon nitride samples were deposited by means of DC magnetron sputtering at room temperature using a power of 200W at 4.5 mTorr. Nitrogen was used as a sputtering gas and varying amounts of argon, between 0 and 10.0 sccm were added. Glass with a thin indium-tin-oxide (ITO), film was used as a substrate (Colorado Concept Coatings). Once grown, x-ray diffraction and raman measurements were taken of the material for structural analysis. Photocurrent spectroscopy was carried out using a set-up containing a light source (tungsten lamp, LPS-220 PTI), which gives light in the visible spectrum; a lock-in amplifier (Stanford research systems SR830 DSP), which measures frequency with which the chopped light passes through to the sample; a potentiostat (Potentiostat/Galvanostat Model 263A), which applies an appropriate potential and measures the current being passed; a monochromator (PTI), that varies the energy of light hitting the sample; and a chopper (Chopper SR540), which regulates the frequency of light allowed to illuminate the sample. Using ocean optics equipment, reflectance and transmission measurements were taken, and initial conductivity measurements were carried out using four-point conductivity (Probe and Hall Probe).

Samples were cut into smaller fractions with a diamond scribe and made into electrodes using front face contact. A top portion of the sample was scraped off and contacted to a copper wire using silver paint (Ted Pella 16034 Colloidal Silver Liquid). The entire assembly was sealed with epoxy leaving only the front surface of the silicon nitride exposed (Loctite 9462 Hysol epoxy adhesive). Surface areas of the electrodes were determined with a photocopy technique which resulted from the ratio of the photocopy area mass to that of a standard 1 cm<sup>2</sup> cutout. Semiconductor characterization was carried out with electrodes submerged in a pH 6 buffer (Metrepack 06914KY), to see whether the open circuit potential became more negative under illumination, or more positive, indicating an n-type semiconductor or a p-type semiconductor.

Using a potentiostat and frequency response analyzer (Solartron 1286 electrochemical interface/SI 1260 Impedance/Gain-Phase Analyzer), various electrochemical measurements were taken using the SiN as the working electrode, a platinum counter electrode, and a silver/silver chloride reference electrode in a 50 mL beaker. Cyclic voltammetry, (I-V), scans were taken in the dark and light (100mW/cm<sup>2</sup>), to see if the material passed anodic or cathodic photocurrent. Mott-Schottky analysis was carried out to determine flat band potentials as well as doping densities. Intensely illuminated open circuit potential measurements were taken using a DC power supply with a tungsten bulb at 10A for determining flatband positions.

Potentiodynamic scans were carried out in 3M H<sub>2</sub>SO<sub>4</sub> (J.T. Baker), pH 7 buffer (Hydriion Buffer Kenvelopes 280-7.00), and 1M KOH (J. T. Baker) under dark and light conditions, for stability assessment, photocurrent response, as well as photovoltage behavior. Electrodes were platinized for further photocurrent analysis using chloroplatinic acid at a coverage of 10mC/cm<sup>2</sup>.

Cyclic voltammetry and potentiodynamic measurement analyses were carried out using CorrWare2 software, and Mott-Schottky analysis was carried out using Zplot software from the vendor Scribner Associates International.

## RESULTS

Photoresponse spectra of the samples were taken and divided by the tungsten lamp spectrum giving a normalized photocurrent response for transmittance and absorbance as seen in Figure 1 and 2, respectively. Samples containing less nitrogen were less transparent and showed more absorbance in the range of 500 to 600 nm, 2.48 to 2.07 eV. Samples containing more nitrogen, more transparent samples, showed less absorbance. Using ocean optics, reflectance and transmission measurements were taken on samples

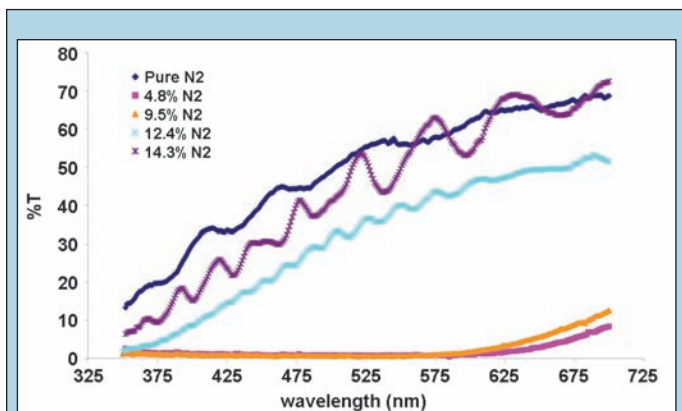


**Figure 1.** Raw transmission data of each sample from 350 to 700 nm using sample as a filter in front of thermopile.

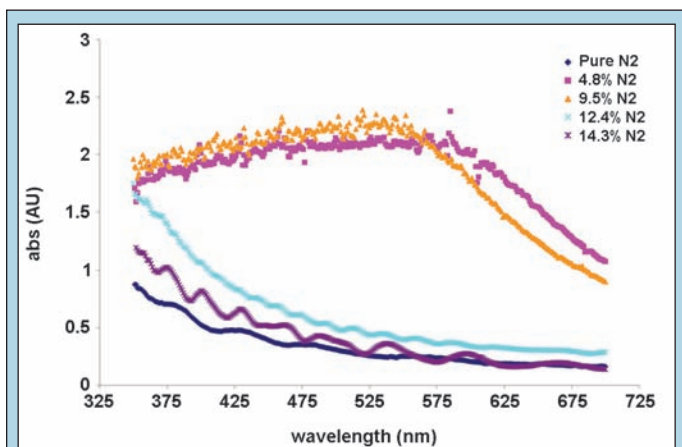


**Figure 2.** Initial absorbance measurements of each sample from 350 to 700 nm at 1 nm steps using the sample as a filter in front of a thermopile normalized to a tungsten lamp spectrum extrapolated from Figure 1.

sputtered with pure  $N_2$  and 4.8%  $N_2$ , as seen in Figure 3 and 4, respectively. This relates to initial absorbance and transmittance measurements giving a bandgap equal to 1.90 eV for the 4.8%  $N_2$  material. X-ray diffraction measurements of the samples showed no peak shifts as compared to ITO as seen in Figure 5. This result indicated amorphous compounds which was further supported by raman analysis.

Preliminary photovoltage shift measurements revealed small changes in electrode potential when illuminated. The largest change in potential occurred for the sample sputtered with 4.8%  $N_2$  giving a potential difference of -131 mV when illuminated as seen in Table 1.

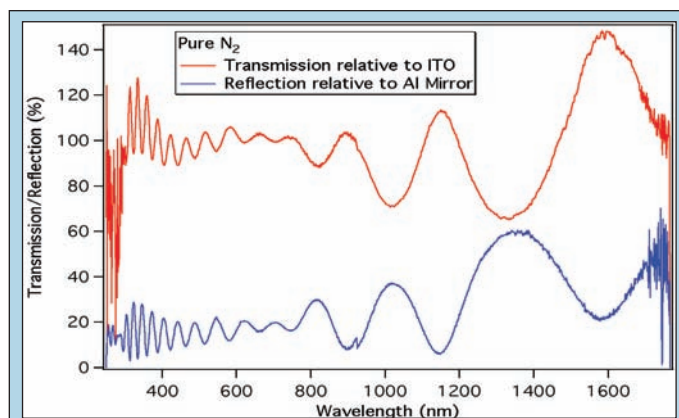


**Figure 3.** Wavelength as a function of percent transmission and reflection of silicon nitride containing pure nitrogen, measured with ocean optic instruments.

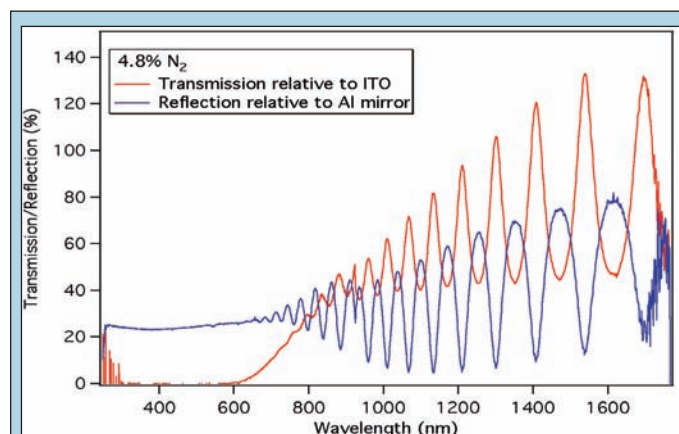


**Figure 4.** Percent transmission and reflection of silicon nitride sample containing 4.8%  $N_2$  using ocean optic instruments.

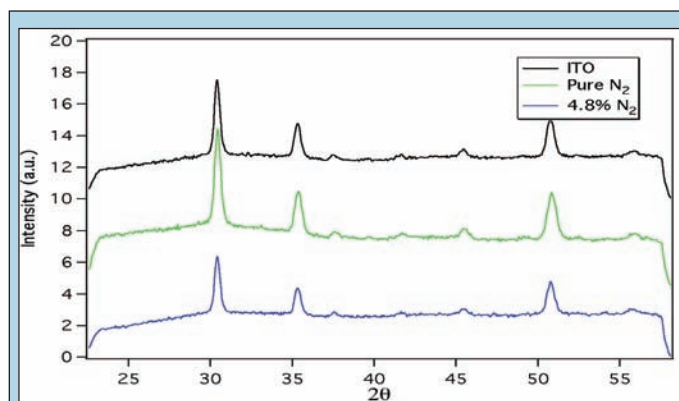


**Figure 5.** X-ray diffraction measurements of ITO as a control, a pure nitrogen sample, and sample containing 4.8%  $N_2$ .

| Sample     | Pure $N_2$ | Pure $N_2$ | Pure $N_2$ | 52.4% $N_2$ | 23.8% $N_2$ | 14.3% $N_2$ | 9.52% $N_2$ | 4.8% $N_2$ |
|------------|------------|------------|------------|-------------|-------------|-------------|-------------|------------|
| Dark       | -0.008     | -0.059     | -0.011     | -0.093      | -0.02       | -0.018      | -0.012      | -0.23      |
| Light      | -0.031     | -0.083     | -0.021     | -0.128      | -0.036      | -0.064      | -0.035      | -0.361     |
| $\Delta V$ | -0.023V    | -0.024V    | -0.01V     | -0.035V     | -0.016V     | -0.046V     | -0.023V     | -0.131V    |

**Table 1.** Open circuit potential measurement changes in pH 6 buffer under dark and light conditions.

Out of the 10 samples deposited by magnetron sputtering, those that were more transparent showed the least photopotential, whereas the less transparent samples showed more change in potential under illumination. All of the samples revealed a more negative potential reading in the light. Four-point conductivity resulted in values greater than  $10^7 \Omega/\text{square}$ .

A sample was submerged in a 50 mL beaker with pH 6 buffer and multiple scans of current versus potential were obtained. Measurements showed a minimal shift in anodic and cathodic current when illuminated for the 10 different batches, including 4.8%  $\text{N}_2$  measurements, as seen in Figure 6. However, when submerged in 3M  $\text{H}_2\text{SO}_4$  the same 4.8%  $\text{N}_2$  sample responded to chopped light, with illumination marked by an increase in cathodic current as seen in Figure 7.

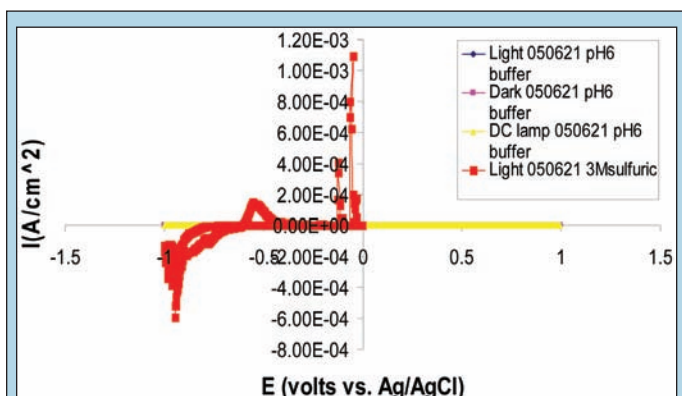


**Figure 6.** I-V cyclic voltammety scan of sample containing 4.8%  $\text{N}_2$  in dark and light conditions with a fiber optic lamp at  $0.100 \text{ W/cm}^2$  in pH 6 buffer and 3M  $\text{H}_2\text{SO}_4$ .

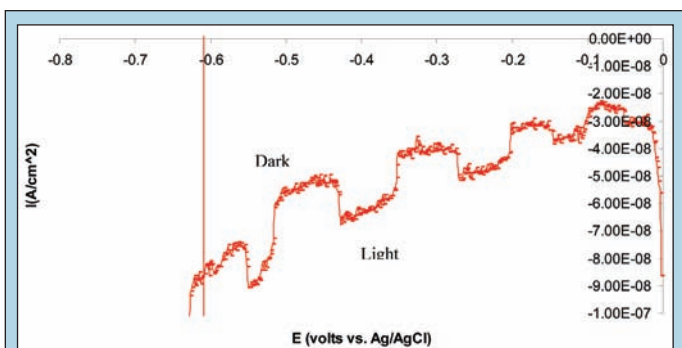


**Figure 7.** I-V scan of sample 4.8%  $\text{N}_2$  in 3M  $\text{H}_2\text{SO}_4$  obtained from hand chop method resulting in a stepwise plot with dark measurements at a lower current and light measurements at the higher cathodic current. Zoomed in from Figure 6.

Varying the frequency between 1000 and 20,000 Hz in the dark and light, while in pH 6 buffer, Mott-Schottky analysis was performed on each sample as seen in Figure 8. All plots obtained from analysis revealed doping densities on the order of  $10^{15}$  to  $10^{17}/\text{cm}^3$ , with varied aphysical x-intercepts, and all positive slopes. Analysis on the 4.8%  $\text{N}_2$  sample revealed flatband potentials near -1.46 V while in pH 6 buffer at 1000 Hz in the light.

Potentiodynamic scans were carried out in acidic, neutral, and basic solutions in the light and dark. As seen in Figure 10, both

anodic and cathodic current increased for the sample sputtered with 4.8%  $\text{N}_2$  when illuminated. Also, there is a drop in the photovoltage when illuminated, and as seen from the plot, low noise activity. Table 2 depicts the intercept values for the current, which are on the order of  $10^{-7} \text{ A/cm}^2$ .

| Sample              | Current (Amps/cm <sup>2</sup> )   |           |           |
|---------------------|-----------------------------------|-----------|-----------|
|                     | 3M H <sub>2</sub> SO <sub>4</sub> | pH 7      | 1M KOH    |
| ITO                 | $10^{-7}$                         | $10^{-8}$ | $10^{-7}$ |
| Pure N <sub>2</sub> | $10^{-8}$                         | $10^{-7}$ | $10^{-7}$ |
| 4.8% N <sub>2</sub> | $10^{-7}$                         | $10^{-8}$ | $10^{-7}$ |

**Table 2.** Current measurements for ITO, pure  $\text{N}_2$ , and 4.8%  $\text{N}_2$  in acidic, neutral, and basic solution when potential is at zero.

## DISCUSSION AND CONCLUSIONS

The absorbance of the sample increases, Figures 1 and 2 show nitrogen content in the sample decreases, as expected from the transparent and nontransparent characteristics of the samples. In Figure 2, the raw absorbance data of the pure nitrogen samples shows minimal absorbance, which would indicate high band gap values for these transparent samples. In contrast, the materials containing 4.8%  $\text{N}_2$  and 14.3%  $\text{N}_2$  show strong absorbance, with a drop off in absorbance near  $\sim 600 \text{ nm}$ , as expected because their red-orange color. These measurements reveal a band gap of  $\sim 2.0 \text{ eV}$ . Further measurements with ocean optics, as seen in Figure 3, show strong correlation in that for the 4.8%  $\text{N}_2$  material the transmission increases at 600 nm giving a band gap equal to 1.90 eV, near the estimated band gap given by photoresponse, and therefore are sufficient for water-splitting. Also, for a sample sputtered with pure nitrogen, in Figure 4, transmission levels remain high across the spectrum, giving a band gap around 4.0 eV, too large of a value to absorb terrestrial radiation.

Figure 5 shows there is good overlap of the x-ray diffraction peaks when looking at the ITO, pure  $\text{N}_2$ , and 4.8%  $\text{N}_2$ . This lack of shift in peaks would suggest that this material is non crystalline and has amorphous qualities. Results from raman analysis show no peak behavior, also suggesting non crystalline material.

From Table 1, multimeter conductivity measurements show small changes in potential under illumination. The four-point conductivity measurements of greater than  $10^7 \Omega/\text{square}$  further support silicon nitride films being a resistive material. Comparing changes in potential it can be seen that the less transparent, 4.8%  $\text{N}_2$  sputtered sample, has the greatest change, -131 mV. Therefore, of these samples, this material has the greatest ability to absorb photons to excite electrons. The common trend of a more negative potential resulting under illumination suggests that silicon nitride behaves as an n-type semiconductor. For n-type semiconductors, the bands bend up at the semiconductor/electrolyte interface. Illuminating the semiconductor and holding the circuit open results in a flattening of the bands which is measured as a negative shift in the Fermi level, or measured potential [4].

I-V plots also give an indication of whether the semiconductor exhibits p-type or n-type behavior, as seen in Figure 6. In comparing

light and dark measurements, minimal photocurrent is generated in pH 6 buffer. However, when the sample is placed in 3M H<sub>2</sub>SO<sub>4</sub>, a photocurrent is observed (Figure 7). For p-type semiconductors, photocurrent is negative because of the orientation of the electric field surface, which is seen in Figure 7, inferring p-type behavior of the 4.8% N<sub>2</sub> sputtered material.

Mott-Schottky analysis is also a good indicator of the type of semiconductor. With Mott-Schottky plots having polarization as a function of the inverse of capacitance squared, it is suggested that for p-type materials that, when there is an increase in negative potential there is an increase in the depletion layer width. This in turn causes the capacitance of the material to decrease, thereby causing 1/C<sup>2</sup> to increase, resulting in a negative slope for the M-S plot as seen in Figure 8. This suggests the silicon nitride as an n-type material, as expected from measurements determined by open circuit potential.

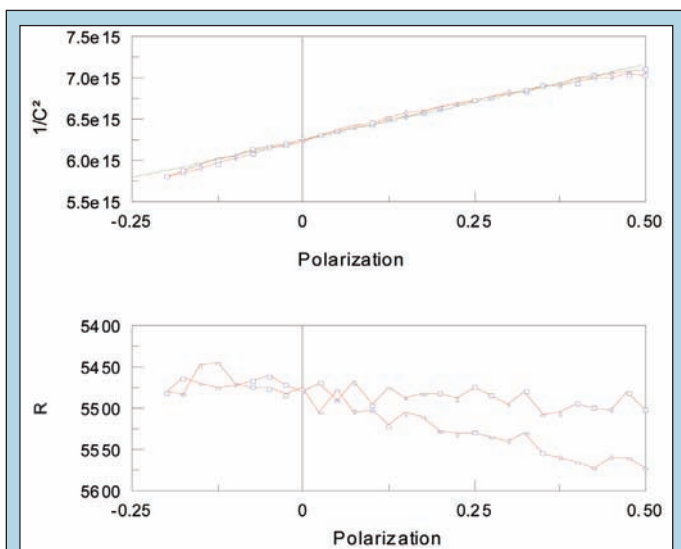


**Figure 8.** Mott-Schottky plot of polarization as a function of the inverse of capacitance squared above and polarization as a function of resistance below with regression performed on above plot.

Mott-Schottky analysis can also indicate where the flatband potential lies as well as the doping density. Performing linear regression on the M-S plot for 4.8% N<sub>2</sub> yields an x-intercept value of -1.46 V. Since the slope of this material indicates n-type behavior, this would suggest the location of the Fermi level, giving an accurate location of the conduction band. From the obtained band gap of 1.90 eV, the valence band is then estimated to be 0.44 V. Because this measurement was carried out in pH 6 buffer, the reduction potential of H<sub>2</sub>O lies at -0.56 V and the oxidation potential lies at 0.67 V. Therefore, even though the band gap of this material is sufficient for splitting water and the conduction band lies more negative of the reduction potential, the valence bands does not lie more positive than the oxidation potential, which suggests that silicon nitride is not capable of splitting water in pH 6 buffer, due to this non band edge “straddling” as seen in Figure 9. Doping densities of all 10 batches of materials were on the order of 10<sup>15</sup> to 10<sup>17</sup>/cm<sup>3</sup>, typical values for a semiconductor.

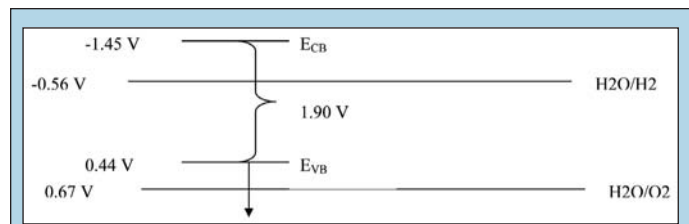


**Figure 9.** Representation of the band edge locations with respect to the redox potentials when submerged in pH 6 buffer. Arrow indicates where energy of valence band should be located.

Potentiodynamic scans, which look at logarithm of current as a function of potential, can be used for stability. Figure 10 shows that when the dark scan and light scan are compared, there is a drop in the photovoltage in the light indicating an n-type material,

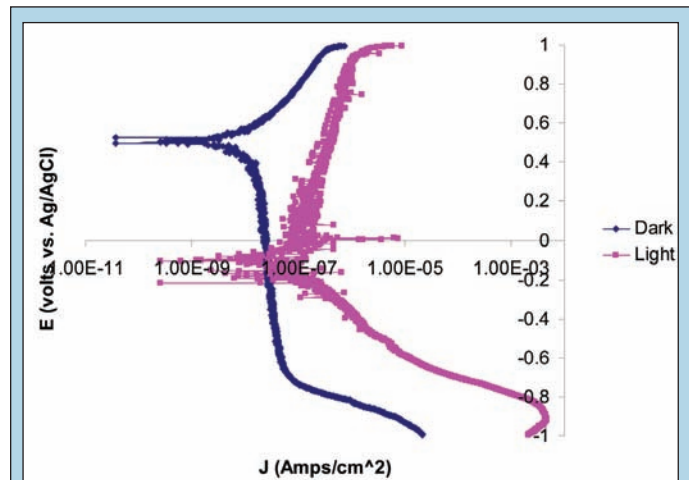


**Figure 10.** Potentiodynamic scan in 3M H<sub>2</sub>SO<sub>4</sub> of sample containing 4.8% N<sub>2</sub> in the dark and light. Light scans show a drop in photovoltage when illuminated, as well as an increase in the anodic and cathodic current from shifts in current both above and below the horizontal peak where the shift from cathodic to anodic current takes place. Stability exhibited in both the dark and light plot.

as expected from open circuit potential measurements. However, when in the light there is an increase in anodic as well as cathodic current, indicating both n-type and p-type behavior when in 3M H<sub>2</sub>SO<sub>4</sub>. This would suggest that the 4.8% N<sub>2</sub> material has intrinsic, or compensated, characteristics.

Table 2 shows that when compared with ITO as a control, samples sputtered with both pure N<sub>2</sub> and 4.8%N<sub>2</sub>, silicon nitride seems to pass a similar current when there is zero potential in the system. This further supports the suggestion that silicon nitride is a resistive material due to it crossing at a low current. Factoring in the low noise level shown in Figure 10, and the low current measurements from Table 2 of both pure N<sub>2</sub> and 4.8% N<sub>2</sub>, silicon nitride appears to be a stable material, characteristic of a protective coating.

In conclusion, the goals of this research were realized in that silicon nitride was studied for its water-splitting and corrosion-protection capabilities. The results of this study suggest that silicon nitride is a resistive material that has intrinsic semiconductor characteristics. Corrosion measurements revealed low current and low noise plots suggesting not only a resistive material, but also a

stable material. With the ability to manufacture transparent silicon nitride, these results will allow for further corrosion and protective coating measurements to be made, such that this material has the potential to solve the problems of using silicon carbide as a protective coating. Future work at NREL will look at possible dopants for the material to enhance the n-type or p-type behavior, as well as growth on other substrates. The stable characteristic of this material needs further quantitative analysis.

#### ACKNOWLEDGEMENTS

This research was conducted at the NREL. I would like to thank the U.S. Department of Energy, Office of Science for the opportunity to participate in the SULI program to further my knowledge of science and renewable energies. I would like to thank Dr. John Turner for his patience, humor, and knowledge of this research. I would also like to thank Todd Deutsch and Jen Leisch for their expertise in this area of research and for taking the time to instruct me on the concepts used in this study. I would also like to thank Maikel van Hest for growing my samples, and my other coworkers in the Electric & Hydrogen Technologies & Systems Center at NREL.

#### REFERENCES

- [1] IPCC Third Assessment Report. 2003.
- [2] Turner, John A. "Photoelectrochemical Water Splitting". 2004 DOE Hydrogen, Fuel Cells & Infrastructure Technologies Program Review. 2004.
- [3] Kocha, Shyam S., Turner John A. "Study of the Schottky barrier and determination of the energetic positions of band edges at the n- and p-type gallium indium phosphide electrode /electrolyte interface". *Journal of Electroanalytical Chemistry*. Vol. 367, 1994 pp. 27-30.
- [4] Bott, Adrian W. "Electrochemistry of Semiconductors". *Current Separations*. Vol. 17, 1998. pp. 87-91.
- [5] Turner, John A. "Energetics of the Semiconductor-Electrolyte Interface". *Journal of Chemical Education*. Vol. 60, 1983 pp.327-329.
- [6] Varner, K. "Evaluation of Amorphous Silicon as a Direct Water Splitting System". 2002 National Renewable Energy Laboratory Internal Report.
- [7] Y. Hirohata. "Properties of silicon nitride films prepared by magnetron sputtering". *Thin Solid Films*. Vol. 253, 1994. pp. 425-429.